Received: 17 March 2017 | Revised: 28 May 2017 | Accepted: 9 June 2017

DOI: 10.1002/aoc.3949

FULL PAPER

WILEY Applied Organometallic Chemistry

Amino acid ionic liquid-based titanomagnetite nanoparticles: An efficient and green nanocatalyst for the synthesis of 1,4-dihydropyrano[2,3-*c*]pyrazoles

Davood Azarifar | Omolbanin Badalkhani | Younes Abbasi

Department of Chemistry, Bu-Ali Sina University, 65178 Hamedan, Iran

Correspondence
Davood Azarifar, Department of Chemistry, Bu-Ali Sina University, 65178 Hamedan, Iran.
Email: azarifar@basu.ac.ir

The amino acid ionic liquid tetrabutylammonium asparaginate (TBAAsp) was immobilized on titanomagnetite ($Fe_{3-x}Ti_xO_4$) nanoparticles in a facile one-pot process using an organosilane compound (TMSP) as spacer. The modified $Fe_{3-x}Ti_xO_4$@TMSP@TBAAsp magnetic nanoparticles were characterized using Fourier transform spectroscopy, scanning electron microscopy, energy-dispersive X-ray spectroscopy, vibrating sample magnetometry and thermogravimetric analysis. The resulting analytical data clearly verified the successful immobilization of the ionic liquid on the magnetic substrate. The magnetic ionic liquid-based nanoparticles exhibited high catalytic activity in the synthesis of 1,4-dihydropyrano[2,3-*c*]pyrazole derivatives via a one-pot three-component reaction under mild reaction conditions. The catalyst was easily recycled and reused for at least six runs without any considerable loss of activity.

KEYWORDS
1,4-dihydropyrano[2,3-*c*]pyrazoles, amino acid ionic liquid, ionic liquid-based magnetic nanocatalyst, one-pot three-component synthesis, titanomagnetite nanoparticles

1 | INTRODUCTION

Recently, nanoparticles have attracted significant interest as efficient catalysts and supports for numerous organic reactions and industrial processes because of their unique size and extraordinary physical and chemical properties including high surface-to-volume ratio and coordinated parts providing a great number of active sites per unit area.[1] Metal oxide nanoparticles with significant magnetic properties have become very attractive due to their role as efficient catalysts and alternatives for the immobilization of a wide range of homogeneous catalysts and ionic liquids (ILs).[2] Nevertheless, these magnetic nanoparticles (MNPs) are aggregated quickly into larger groupings and thereby lose their unique properties. As an effective protection strategy, covalent linkage of organic or inorganic molecules such as organosilanes to MNPs has been used to prevent their easy oxidation and also aggregation and to preserve their unique magnetism and dispersibility. In addition, organofunctional alkoxysilane linkers act to provide silicon coating of nanoparticles in order to maintain chemical stability and provide reactive sites on the surface of the nanoparticles for efficient grafting of different groups on their surface.[3,4]

ILs have become attractive as environmentally friendly reaction media and catalysts and have been widely used in organic reactions due to their environmental benignity, high thermal stability, reusability, negligible vapour pressure and easy handling.[5–7] Despite promising advantages, ILs have disadvantages including high viscosity resulting in decreased catalytic activity and homogeneous behaviour in reactions making product separation and catalyst recovery more complicated. To solve such problems, immobilization of

ILs onto various nanosized solid supports, especially magnetic nanomaterials, has been the most promising solution. The obtained IL-based heterogeneous nanocatalysts possess advantages including reusability, easy separation, enhanced stability and catalytic activity along with retaining the above-mentioned physical and chemical properties.[8–11]

Among nanomaterials employed as supports for various catalysts and ILs, MNPs have become popular due to their high stability, easy synthesis and functionalization and high surface area.[12–16] Furthermore, MNPs can be simply separated from a reaction mixture by applying an external magnetic field. This strategy is more efficient compared to tedious isolation processes such as filtration or centrifugation.

Considering the advantages of IL-immobilized MNPs as designable catalysts, such as environmental friendliness, easy separation and reusability, non-volatility, high catalytic efficiency and high thermal stability, we used $Fe_{3-x}Ti_xO_4$ MNP-supported tetrabutylammonium asparaginate (TBAAsp) IL as an efficient catalyst for the synthesis of dihydropyrano[2,3-*c*]pyrazoles via environmentally benign multi-component reactions (Scheme 1). Recently, multi-component reactions have become popular as an atom-economic concept because products can be obtained with a single-step reaction and a variety of products can be obtained by changing the reaction components.[17–19]

Dihydropyrano[2,3-*c*]pyrazoles and their derivatives are widely used in synthetic organic and bioorganic chemistry because of their pharmacological and therapeutic properties including insecticidal, diuretic, anticoagulant, anticancer, antibacterial, analgesic and anti-inflammatory activities.[20] There are numerous synthetic procedures available for the synthesis of 1,4-dihydropyrano[2,3-*c*]pyrazole derivatives using various catalytic systems and application of multi-component reactions under a variety of conditions.[21–25]

2 | EXPERIMENTAL

2.1 | Materials and instrumentation

Melting points were determined in open capillaries with a Buchi 510 apparatus. Fourier transform infrared (FT-IR) spectra were recorded in KBr pellets with a Shimadzu 435-U-04 FT-IR spectrometer. ^{1}H NMR and ^{13}C NMR spectra were obtained with 250 and 400 MHz Bruker Avance instruments in DSMO-d_6 as a solvent and tetramethylsilane as an internal standard. Energy-

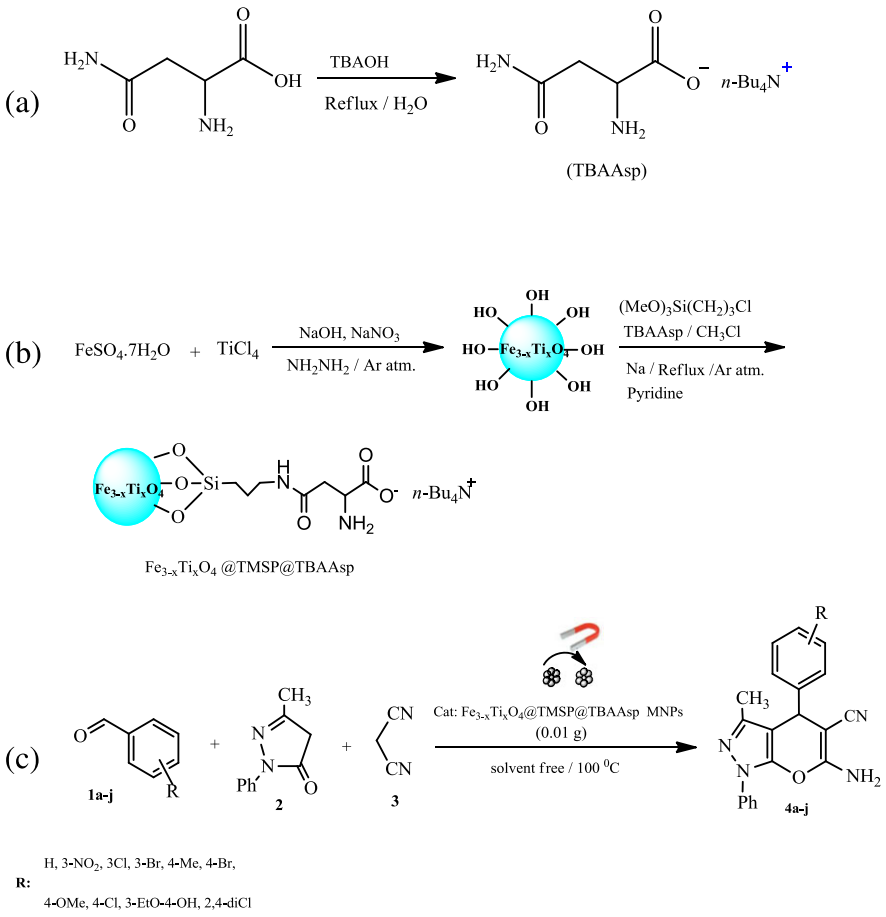

SCHEME 1 (a) Synthesis of amino acid IL (TBAAsp). (b) Synthesis of $Fe_{3-x}Ti_xO_4$@TMSP@TBAAsp catalyst. (c) Synthesis of 1,4-dihydropyrano[2,3-*c*] pyrazole derivatives **4a–j** catalysed by $Fe_{3-x}Ti_xO_4$@TMSP@TBAAsp

dispersive X-ray (EDX) analysis was conducted with a SAMX instrument. Scanning electron microscopy (SEM) images were obtained with a KYKYEM-3200 instrument operated at an accelerating voltage of 26 kV. Magnetic susceptibility measurements were performed at room temperature with a vibrating sample magnetometry (VSM) instrument (model MDKFT). To investigate thermal stability, thermogravimetric analysis (TGA) was performed with a TGA/DTA Linseis-181a1750 instrument at a heating rate of 5°C min^{-1} in the range 25–1000°C under nitrogen flow. Ultrasonication was performed using a 2200 ETH-SONICA ultrasound cleaner with a frequency of 45 kHz. Mass spectra were recorded with a FINNIGAN-MAT 8430 spectrometer operating at an ionization potential of 70 eV.

2.2 | Preparation of TBAAsp IL

TBAAsp IL was fabricated following a modified procedure reported previously[26] (Scheme 1a). A solution of L-asparagine amino acid (2.64 g, 20 mmol) in 20 ml of distilled water was ultrasonicated for 20–30 min at room temperature to give an aqueous suspension. Then, 5.2 ml (20 mmol) of 40% aqueous tetrabutylammonium hydroxide was added and the resulting mixture was stirred vigorously under reflux condition for 24 h. Following water removal in air, 10 ml of chloroform was added to the reaction mixture containing unreacted asparagine amino acid and desired IL. Finally, the remaining amino acid was separated by filtration and the filtrate was dried in air to afford the yellow viscous IL. The spectral (^{1}H NMR, ^{13}C NMR and MS) data for the sample are presented in the supporting information.

TBAAsp IL. Yellow viscous liquid. IR (KBr, ν, cm^{-1}): 3383, 3295, 2967, 2941, 2875, 1667, 1578, 1490, 1468, 1366. ^{1}H NMR (400 MHz, DMSO-d_6, δ, ppm): 0.95 (t, $12H_a$, $4CH_3$), 1.31–1.33 (m, $8H_b$, $4CH_2$), 1.58 (m, $8H_c$, $4CH_2$), 1.88–1.95 (dd, 1H, $H_2NOC\text{-}CH_f$), 2.42–2.43 (dd, 1H, $H_2NOC\text{-}CH_e$), 3.17–3.22 (m, $8H_d$, $4CH_2$), 3.59 (dd, $1H_g$, $CHNH_2$), 5.1, 6.32 (4H, $2NH_2$). ^{13}CNMR (400 MHz, DMSO-d_6, δ, ppm): 13.9 (C_aH_3), 19.7 (-C_bH_2), 23.6 (-C_cH_2), 44.3 (C_hH_2), 54.2 (HC_g-NH_2), 57.9 (-C_dH_2), 174.9 (OC_e-NH_2), 175.4 (C_fOO^-). MS (70 eV): m/z = 373.4.

2.3 | Fabrication of $Fe_{3-x}Ti_xO_4$ MNPs

Titanomagnetite nanoparticles were fabricated according to our previously reported approach.[22] In a flask, 3.81 g (13.6 mmol) of $FeSO_4{\cdot}7H_2O$ was dissolved in 18 ml of deionized water. The pH of the solution was adjusted to less than 1 by adding 1 M HCl (7 ml) solution. Then, 1.6 ml of $TiCl_4$ and 2 ml of hydrazine monohydrate were added dropwise to the reaction mixture. The resulting mixture was refluxed at 90°C for 30 min under nitrogen atmosphere. Then, aqueous solutions of 4 g of NaOH and 2 g of $NaNO_3$ in 18 ml of deionized water were added to the mixture and refluxed under vigorous stirring for 1 h. Finally, the reaction mixture was cooled to room temperature to precipitate titanomagnetite nanoparticles which were separated using a magnetic bar, washed with water and dried in air.

2.4 | Preparation of $Fe_{3-x}Ti_xO_4$@TMSP@TBAAsp catalyst

The surface of the synthesized MNPs ($Fe_{3-x}Ti_xO_4$) was functionalized using 3-chloropropyltrimethoxysilane (CPTMS) and TBAAsp IL using a facile one-pot process. MNPs (0.61 g) were dispersed in 20 ml of pyridine under ultrasonication for 30 min. Then, a small amount of sodium metal, 1 ml (5.5 mmol) of CPTMS and a solution of 2.04 g (5.5 mmol) of TBAAsp in 5 ml of chloroform were added into the reaction mixture under argon atmosphere and the obtained mixture was ultrasonicated for a further 15 min. Then, the mixture was stirred under reflux condition at 110°C for 24 h. The precipitated nanoparticles were separated using a magnetic bar, washed with ethanol and dried in air to afford about 1.4 g of light brown powder.

2.5 | Determination of pH value of catalyst

A simple procedure was used for the determination of the pH value of the catalyst. A mixture of 0.05 g of the $Fe_{3-x}Ti_xO_4$@TMSP@TBAAsp catalyst in distilled water (10 ml) was stirred at room temperature for 24 h. Then, the pH value of the resulting mixture was measured using a pH meter (Metrohm 827, Herisan, Switzerland) with a combined glass electrode). As expected, the measured pH value was found to be 9.37 confirming that the synthesized catalyst is a basic composite compound. This result could be explained by the presence of two amine groups in the grafted TBAAsp IL moiety and the remaining unreacted hydroxyl groups on the surface of the catalyst.

2.6 | Typical procedure for synthesis of 1,4-Dihydropyrano[2,3-*c*]pyrazoles

In a flask containing 0.01 g of $Fe_{3-x}Ti_xO_4$@TMSP@TBAAsp catalyst were added aldehyde (1 mmol), malononitrile (1 mmol) and 3-methyl-1-phenyl-1*H*-2-pyrazol-5(4*H*)-one (1 mmol) under solvent-free conditions. The reaction mixture was stirred at 100°C for an appropriate time. Once the reaction was completed, as monitored by

TLC, the mixture was cooled to room temperature, diluted with 10 ml of ethanol and stirred for 10 min. Then, an external magnetic field was applied to separate the catalyst, and the remaining solution was evaporated. The precipitated solid product was recrystallized from ethanol to yield pure product. All the synthesized products **4a–j** were known compounds which were characterized by their melting points and spectral (FT-IR, ^{1}H NMR and ^{13}C NMR) data and compared with the corresponding reported data.

2.6.1 | 6-Amino-3-methyl-1,4-diphenyl-1,4-dihydropyrano[2,3-c]pyrazole-5-carbonitrile (4a)

White solid; yield: 0.295 g (90%); m.p. 170–173°C. IR (KBr, ν, cm^{-1}): 3472, 3324, 3194, 3063, 2923, 2198, 1659, 1625, 1592, 1516, 1386, 1265, 1126, 754. ^{1}H NMR (90 MHz, $CDCl_3$, δ, ppm): 1.89 (t, 3H, CH_3), 4.66–4.69 (3H, CH and NH_2), 7.28–7.61 (m, 10H, H-Ar). ^{13}C NMR (100 MHz, DMSO-d_6, δ, ppm): 13.0, 37.2, 58.7, 99.1, 116.5, 120.4, 126.6, 127.5, 128.2, 128.9, 129.7, 137.9, 144.0, 144.3, 145.7, 159.8.

2.6.2 | 6-Amino-3-methyl-4-(3-nitrophenyl)-1-phenyl-1,4-dihydropyrano[2,3-c]pyrazole-5-carbonitrile (4b)

Cream solid; yield 0.332 g (89%); m.p. 191–193°C. IR (KBr, ν, cm^{-1}): 3439, 3300, 3191, 3101, 2195, 1649, 1592, 1387, 1263, 1123, 1071, 754. ^{1}H NMR (250 MHz, DMSO-d_6, δ, ppm): 1.77 (s, 3H, CH_3), 4.93 (s, 1H, CH), 7.29–7.78 (m, 9H, H-Ar), 8.13 (s, 2H, NH_2). ^{13}C NMR (100 MHz, DMSO-d_6, δ, ppm): 13.1, 35.6, 56.1, 96.6, 120.5, 121.7, 121.9, 130.2, 134.3, 135.9, 146.8, 147.8, 154.6, 160.1.

2.6.3 | 6-Amino-4-(3-chlorophenyl)-3-methyl-1-phenyl-1,4-dihydropyrano[2,3-c]pyrazole-5-carbonitrile (4c)

White solid; yield 0.323 g (89%); m.p. 159–162 °C. IR (KBr, ν, cm^{-1}): 3463, 3319, 2193, 1655, 1594, 1391, 1265, 1126, 1070, 756. ^{1}H NMR (400 MHz, DMSO-d_6, δ, ppm): 1.81 (s, 3H, CH_3), 4.76 (s, 1H, CH), 7.25–7.81 (m, 10H, H-Ar and NH_2). ^{13}C NMR (100 MHz, DMSO-d_6, δ, ppm): 13.1 (CH_3), 36.9 (CH), 57.9 (C-CN), 98.4 (CN), 120.3, 120.5, 126.7, 127.1, 127.6, 128.0, 129.8, 130.9, 133.6, 137.9, 144.4, 145.6, 146.7, 160.01, 160.05.

2.6.4 | 6-Amino-4-(3-bromophenyl)-3-methyl-1-phenyl-1,4-dihydropyrano[2,3-c]pyrazole-5-carbonitrile (4d)

White solid; yield 0.358 g (88%); m.p. 162–165°C. IR (KBr, ν, cm^{-1}): 3453, 3337, 3194, 2823, 2194, 1655, 1591, 1519, 1390, 1127, 1071, 754. ^{1}H NMR (400 MHz, DMSO-d_6, δ, ppm): 1.81 (s, 3H, CH_3), 4.75 (s, 1H, CH), 7.29–7.81 (m, 10H, H-Ar and NH_2). ^{13}C NMR (100 MHz, DMSO-d_6, δ,ppm): 13.1, 36.8, 57.9, 98.4, 120.3, 120.5, 122.3, 126.7, 127.5, 129.8, 130.5, 130.9, 135.0, 131.2, 137.9, 144.4, 145.6, 146.9, 160.02, 160.06.

2.6.5 | 6-Amino-4-(2,4-dichlorophenyl)-3-methyl-1-phenyl-1,4-dihydropyrano[2,3-c]pyrazole-5-carbonitrile (4e)

Yellow solid; yield 0.353 g (89%); m.p. 184–187°C. IR (KBr, ν, cm^{-1}): 3458, 3325, 2199, 1660, 1591, 1520, 1393, 1269, 1126, 1072, 758. ^{1}H NMR (90 MHz, $CDCl_3$, δ, ppm): 1.78 (s, 3H, CH_3), 5.16 (s, 1H, CH), 7.32–7.80 (m, 10H, H-Ar and NH_2). ^{13}C NMR (100 MHz, DMSO-d_6, δ, ppm): 12.8, 34.0, 56.62, 97.77, 120.0, 120.5, 126.7, 128.6, 129.4, 129.8, 132.9, 133.0, 133.5, 137.9, 139.7, 144.7, 145.3, 160.3, 160.4.

2.6.6 | 6-Amino-4-(4-methoxyphenyl)-3-methyl-1-phenyl-1,4-dihydropyrano[2,3-c]pyrazole-5-carbonitrile (4f)

White solid; yield 0.315 g (88%); m.p. 177–180°C. IR (KBr, ν, cm^{-1}): 3393, 3323, 3205, 2192, 1661, 1596, 1513, 1393, 1250, 1128, 1074, 813, 759. ^{1}H NMR (90 MHz, DMSO-d_6, δ, ppm): 1.78 (s, 3H, CH_3), 3.74 (s, 3H, CH_3), 4.62 (s, 1H, CH), 6.84–7.82 (m, 11H, H-Ar and NH_2). ^{13}C NMR (100 MHz, DMSO-d_6, δ, ppm): 12.3, 38.1, 54.6, 59.1, 98.2, 113.4, 119.7, 125.5, 128.4, 128.8, 134.9, 137.4, 143.5, 145.2, 158.0, 158.9.

2.6.7 | 6-Amino-4-(3-ethoxy-4-hydroxyphenyl)-3-methyl-1-phenyl-1,4-dihydropyrano[2,3-c]pyrazole-5-carbonitrile (4i)

Yellow solid; yield 0.334 g (86%); m.p. 186–190°C. IR (KBr, ν, cm^{-1}): 3420, 3328, 3203, 2923, 2195, 1659, 1596, 1514, 1391, 1273, 1125, 758. ^{1}H NMR (400 MHz, DMSO-d_6, δ, ppm): 1.29–1.33 (t, 3H, CH_3), 1.83 (s, 3H, CH_3), 3.96–4.01 (q, 2H, CH_2), 4.57 (s, 1H, CH), 6.61–7.80 (m, 10H, H-Ar and NH_2), 8.85 (s, 1H, OH). ^{13}C NMR (100 MHz, DMSO-d_6, δ, ppm): 13.1, 15.1, 36.7, 59.1, 64.4,

99.4, 113.9, 115.9, 120.3, 120.6, 126.5, 129.8, 135.0, 138.1, 144.2, 145.0, 146.1, 146.3, 146.8, 146.9, 159.6, 159.7.

2.6.8 | 6-Amino-3-methyl-4-(4-chlorophenyl)-1-phenyl-1,4-dihydropyrano[2,3-c]pyrazole-5-carbonitrile (4j)

White solid; yield 0.341 g (94%); m.p. 178–181°C. IR (KBr, ν, cm^{-1}): 3457, 3326, 3259, 3198, 3067, 2920, 2203, 1663, 1594, 1518, 1393, 1127, 752. ^{1}H NMR (400 MHz, DMSO-d_6, δ, ppm): 1.80 (s, 3H, CH_3), 4.74 (s, 1H, C-H), 7.28–7.81 (m, 11H, H-Ar and NH_2). ^{13}C NMR (100 MHz, DMSO-d_6, δ, ppm): 13.0, 36.5, 58.2, 98.6, 120.3, 120.4, 120.5, 126.7, 129.0, 130.2, 132.1, 137.9, 143.1, 144.4, 145.6, 159.91, 159.95.

3 | RESULTS AND DISCUSSION

3.1 | Characterization of $Fe_{3-x}Ti_xO_4$@TMSP@TBAAsp

Following our previous research, herein we synthesized the hitherto unreported $Fe_{3-x}Ti_xO_4$@TMSP@TBAAsp (Scheme 1b) and investigated its catalytic capability for the synthesis of 1,4-dihydropyrano[2,3-*c*]pyrazole derivatives (Scheme 1c). Interestingly, the presence of Ti^{4+} cations in the structure of the nanoparticles increases

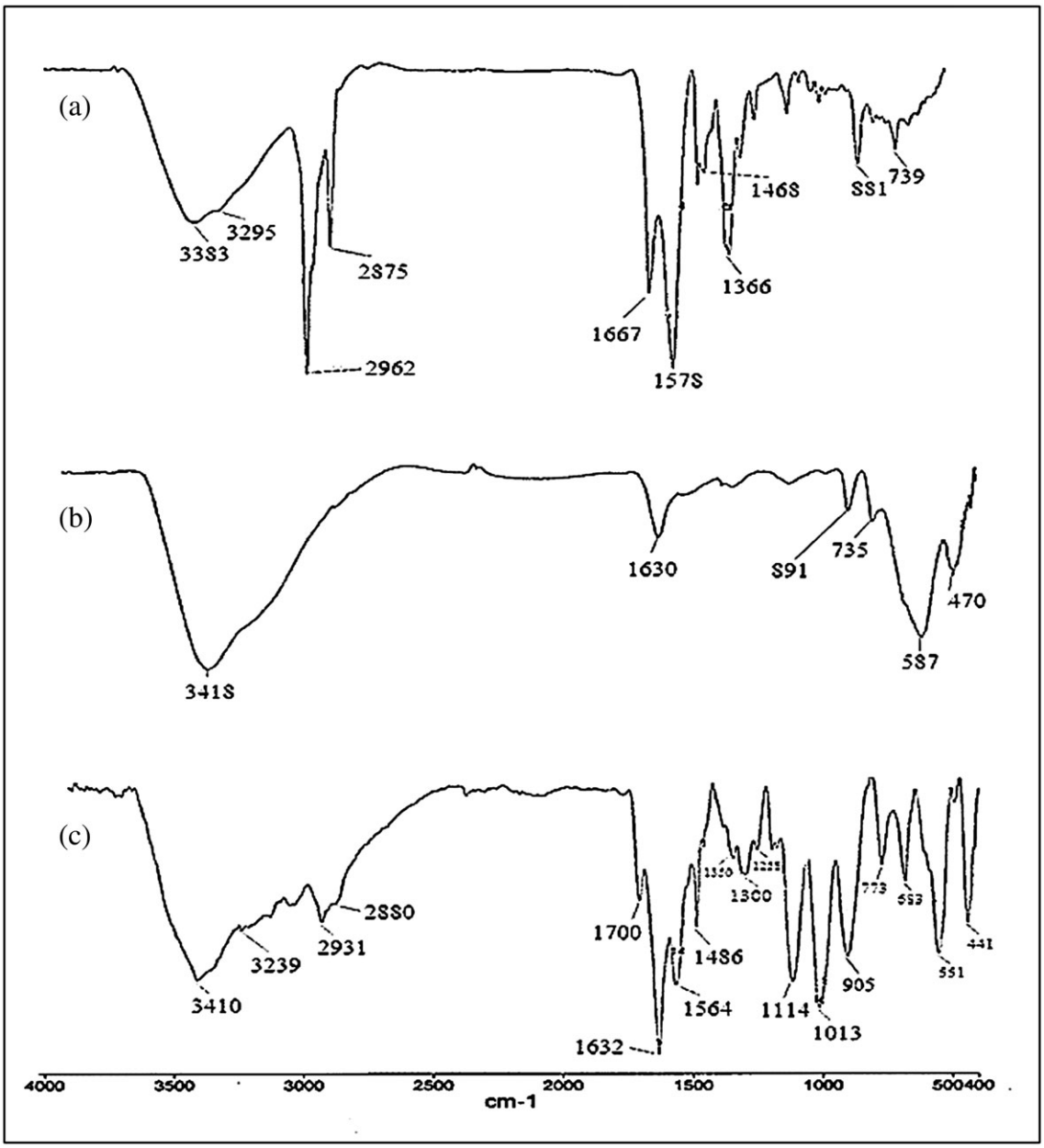

FIGURE 1 FT-IR spectra of (a) TBAAsp, (b) $Fe_{3-x}Ti_xO_4$ MNPs and (c) $Fe_{3-x}Ti_xO_4$@TMSP@TBAAsp MNPs

the number of surface hydroxyl groups.[27] This structural modification improves the loading capacity of the grafted functional groups on the surface of titanomagnetite nanoparticles[22,28] compared with magnetite (Fe_3O_4) nanoparticles.[29,30]

As depicted in Scheme 1(a), first we prepared $Fe_{3-x}Ti_xO_4$ MNPs based on our previously reported approach.[22] A mixture of equimolar amounts of $FeSO_4{\cdot}7H_2O$ and $TiCl_4$ in acidic solution was reacted with hydrazine hydrochloride in deionized water under reflux in nitrogen atmosphere. The produced $Fe_{3-x}Ti_xO_4$ MNPs were magnetically separated from the reaction mixture. Then, the surface of $Fe_{3-x}Ti_xO_4$ MNPs was silylated via a one-pot process with CPTMS to prevent aggregation followed by functionalization with TBAAsp IL in the presence of a small amount of metallic sodium in chloroform under reflux (Scheme 1b). The precipitated $Fe_{3-x}Ti_xO_4$@TMSP@TBAAsp MNPs were magnetically isolated using a magnetic bar. The structure of the synthesized $Fe_{3-x}Ti_xO_4$@TMSP@TBAAsp catalyst was characterized using various analytical techniques such as FT-IR spectroscopy, EDX, SEM, TGA and VSM.

The FT-IR spectra of TBAAsp IL, $Fe_{3-x}Ti_xO_4$ MNPs and $Fe_{3-x}Ti_xO_4$@TMSP@TBAAsp MNPs are presented in Figure 1. Successful functionalization of $Fe_{3-x}Ti_xO_4$ MNPs is verified by comparison between the FT-IR spectra. The bands at 3383, 3295 and 2875–2962 cm^{-1} in the spectrum of the IL (Figure 1a) are attributed to the stretching vibrations of NH_2 and C-H groups. The absorption bands at 1667 and 1578 cm^{-1} are due to the stretching vibrations of C=O bond in amide and carboxylate moieties, respectively. The FT-IR spectrum of $Fe_{3-x}Ti_xO_4$ MNPs (Figure 1b) exhibits characteristic broad absorption bands at 3418 and 1630 cm^{-1} which can be assigned to the asymmetric and symmetric stretching vibrations of O-H bonds, respectively, which are bonded to the surface metal atoms. The bands at 735 and 587 cm^{-1} are due to the symmetric stretching vibrations of Ti-O and Fe-O, respectively. The FT-IR spectrum of $Fe_{3-x}Ti_xO_4$@TMSP@TBAAsp MNPs (Figure 1c) shows stretching vibrational peaks at 3410 and 3239 cm^{-1} (NH), 2864 and 2934 cm^{-1} (C-H), 1700 cm^{-1} (C=O of amide), 1632 cm^{-1} (NH), 1564 cm^{-1} (C=O of carboxylate), 1300 cm^{-1} (C-N), 1114 and 1013 cm^{-1} (Si-O-Si). These results clearly indicate that the surfaces of $Fe_{3-x}Ti_xO_4$ MNPs are successfully functionalized.

The elemental composition of the $Fe_{3-x}Ti_xO_4$@TMSP@TBAAsp MNPs was established using EDX spectroscopy. As shown in Figure 2, the EDX pattern obtained from a typical sample obviously indicates the expected components (C, N, O, Si, Ti, Fe) and good dispersion of the $Fe_{3-x}Ti_xO_4$@TMSP@TBAAsp MNPs.

The sizes and morphologies of $Fe_{3-x}Ti_xO_4$@TMSP@TBAAsp MNPs were investigated using SEM, as shown in Figure 3. It can be seen that the size of these nanoparticles is about 47 nm. The change of particle size from 22 nm in $Fe_{3-x}Ti_xO_4$ MNPs to 47 nm in $Fe_{3-x}Ti_xO_4$@TMSP@TBAAsp MNPs clearly indicates the successful surface functionalization of $Fe_{3-x}Ti_xO_4$ MNPs. Also, SEM micrographs reveal that there are major morphological changes in non-functionalized titanomagnetite nanoparticles compared to the magnetic IL-based nanoparticles.[31]

Magnetic measurements of $Fe_{3-x}Ti_xO_4$ and $Fe_{3-x}Ti_xO_4$@TMSP@TBAAsp were conducted using a VSM instrument at 300 K. The magnetization curves obtained for these nanoparticles are compared in Figure 4. The values of the saturation magnetization for $Fe_{3-x}Ti_xO_4$ and $Fe_{3-x}Ti_xO_4$@TMSP@TBAAsp are 33.85 and 14.05 emu g^{-1}, respectively, at +1000 Oe. The

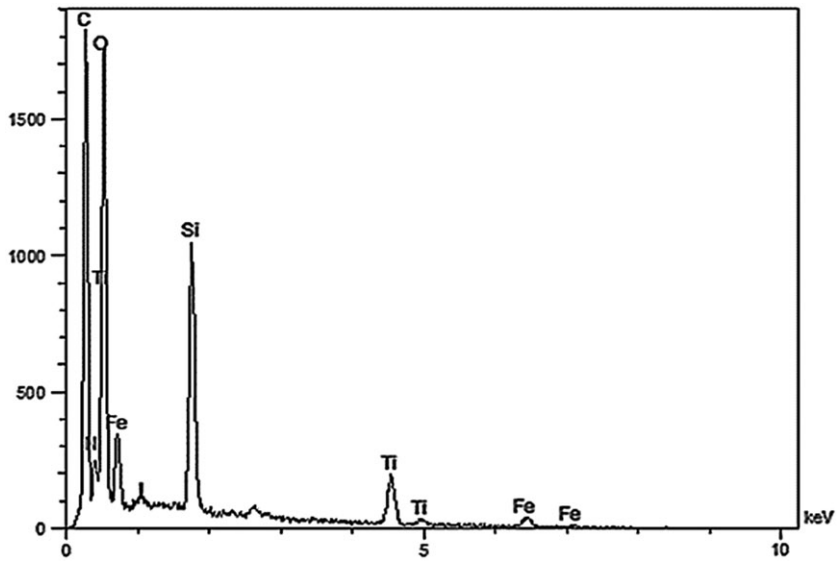

FIGURE 2 EDX pattern of $Fe_{3-x}Ti_xO_4$@TMSP@TBAAsp MNPs

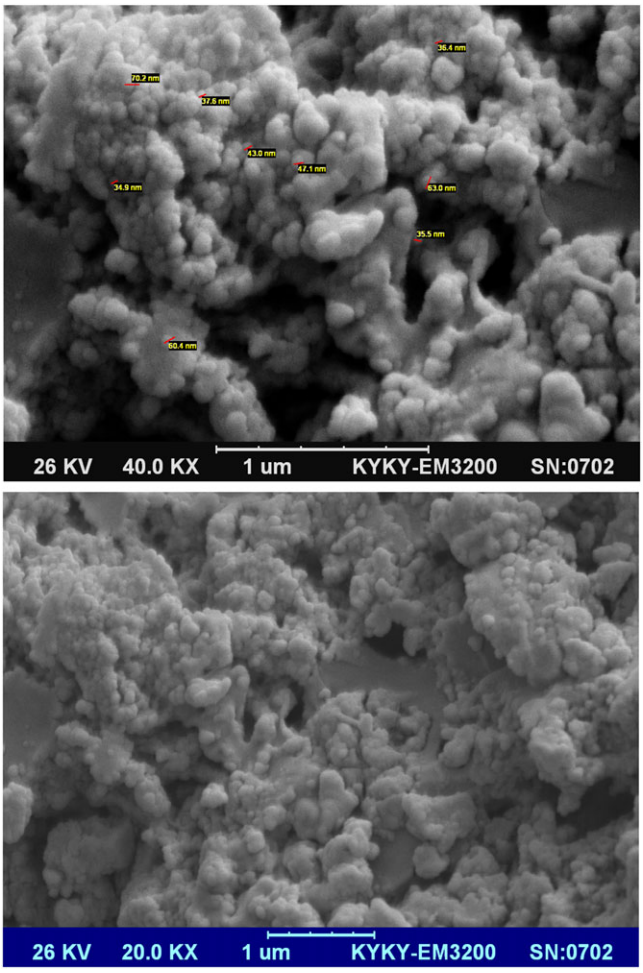

FIGURE 3 SEM images of $Fe_{3-x}Ti_xO_4$@TMSP@TBAAsp MNPs

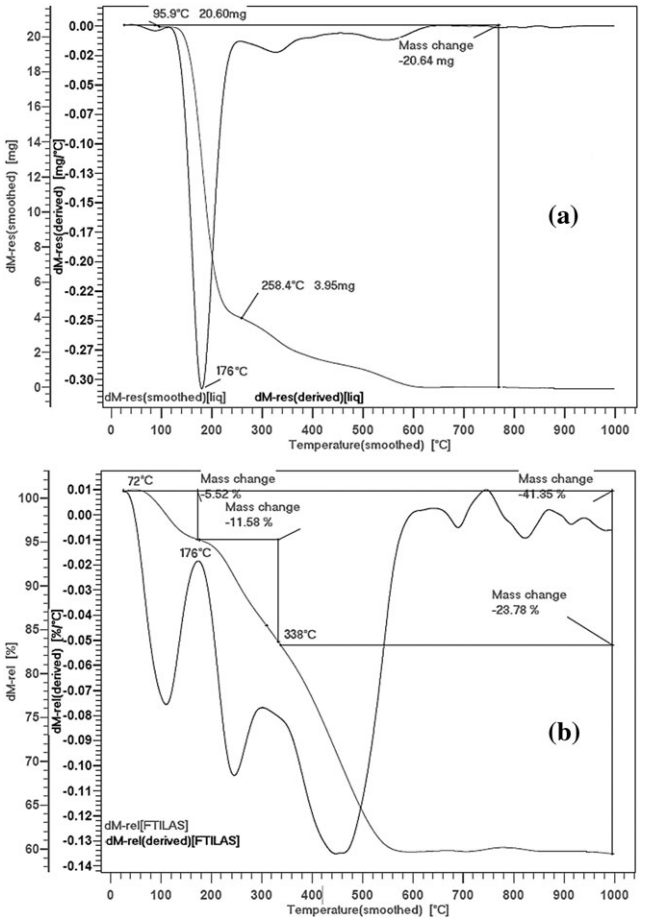

FIGURE 5 TGA and DTA curves of (a) TBAAsp and (b) $Fe_{3-x}Ti_xO_4$@TMSP@TBAAsp MNPs

reduction in the saturation magnetization provides evidence for successful formation of the $Fe_{3-x}Ti_xO_4$@TMSP@TBAAsp MNPs. Even with this reduction in the saturation magnetization, the catalyst can still be efficiently separated from a solution simply by applying an external magnetic field.

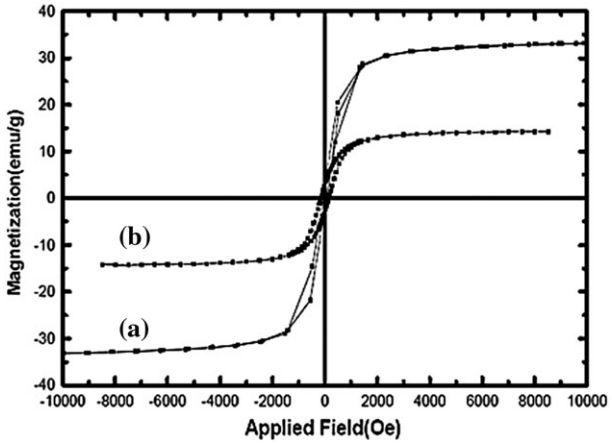

FIGURE 4 VSM patterns of (a) $Fe_{3-x}Ti_xO_4$ MNPs and (b) $Fe_{3-x}Ti_xO_4$@TMSP@TBAAsp MNPs

TGA and derivative thermogravimetric analysis (DTA) of TBAAsp and $Fe_{3-x}Ti_xO_4$@TMSP@TBAAsp MNPs were carried out and their thermal decomposition profiles were obtained as shown in Figure 5. According to Figure 5(a), a considerable weight loss (80.90%) occurs at 95–258°C (centred at 176°C) which is attributed to the weight loss in the synthesized IL sample (TBAAsp) and further increasing the temperature from 258 to 580°C brings about the complete decomposition of the corresponding IL compound. Also, the TGA thermogram of $Fe_{3-x}Ti_xO_4$@TMSP@TBAAsp MNPs (Figure 5b) shows a weight loss of 5.52% at 72–176°C (centred at 110°C) which can be attributed to the removal of residual water, other solvents and remaining hydroxyl groups on the catalyst surface. A significant weight loss of about 11.58% occurs in the second stage at 176–338°C (centred at 258°C) which could be due to the removal of the immobilized IL (TBAAsp) and organosilane spacer groups (TMSP) grafted on the surface of $Fe_{3-x}Ti_xO_4$ MNPs. The third weight loss occurs at 338–600°C (centred at 450°C) and probably results from the complete decomposition of $Fe_{3-x}Ti_xO_4$ MNPs. Therefore, according to the obtained results, the

thermal stability of the synthesized IL (TBAAsp) was calculated to be about 258°C. In addition, our synthesized catalyst exhibits a higher grafting capacity of the IL on the surface of the titanomagnetite nanoparticles (11.58%) in comparison to previously reported similar magnetite (Fe_3O_4) nanoparticles grafted with another IL (6.1%).[32]

3.2 | Evaluation of catalytic activity of $Fe_{3-x}Ti_xO_4$@TMSP@TBAAsp in synthesis of 1,4-Dihydropyrano[2,3-*c*]pyrazole derivatives

In view of the beneficial applications of IL-based heterogeneous catalysts in organic reactions, we were encouraged to prepare $Fe_{3-x}Ti_xO_4$@TMSP@TBAAsp as a new basic IL magnetite and examine its catalytic activity in the synthesis of dihydropyrano[2,3-*c*]pyrazoles under solvent-free conditions. The one-pot three-component reaction between benzaldehyde, malononitrile and 3-methyl-1-phenyl-1*H*-2-pyrazol-5(4*H*)-one was chosen as model reaction. The impacts of reaction parameters such as solvent (EtOH, H_2O), catalyst loading and temperature were analysed, as summarized in Table 1. The best results in terms of reaction yield and time are obtained when the reaction is performed at 100 °C under solvent-free conditions in the presence of 0.01 g of catalyst (entry 8). It is observed that higher amounts of catalyst at 100°C under solvent-free conditions inhibit the formation of the product (entries 9–11). The catalytic activity of $Fe_{3-x}Ti_xO_4$@TMSP@TBAAsp was evaluated by performing a similar reaction in the absence of the catalyst which gives only a trace amount of product (entry 13).

The generality and scope of the proposed reaction was extended by using a diverse series of aromatic aldehydes **1a–j** bearing various substituents under the above-mentioned optimal conditions. On the basis of the results summarized in Table 2, the reactions proceed smoothly to furnish the relevant products in high yields (90–96%) and short reaction times (15–60 min) regardless of the substituent nature. The obtained products are all known compounds and were characterized based on their physical and spectral (FT-IR, ^{1}H NMR and ^{13}C NMR) data and compared with corresponding reported data (Table 2).

3.3 | Catalytic reaction mechanism

A reasonable mechanism is proposed to describe the one-pot three-component reaction between aromatic aldehydes, malononitrile and 3-methyl-1-phenyl-1*H*-2-pyrazol-5(4*H*)-one in the presence of $Fe_{3-x}Ti_xO_4$@TMSP@TBAAsp as a basic catalyst as depicted in Scheme 2. First, the catalyst accelerates the deprotonation of malononitrile into relevant anion which

TABLE 1 Screening reaction parameters for synthesis of 6-amino-3-methyl-1,4-diphenyl-1,4-dihydropyrano[2,3-*c*]pyrazole-5-carbonitrile[a]

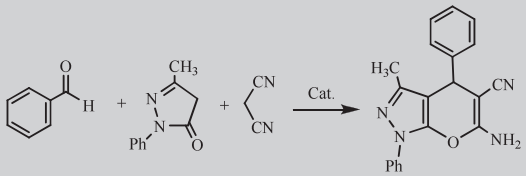

Entry	Catalyst (g)	Solvent	Temperature (°C)	Time (min)	Yield (%)[b]
1	0.01	H_2O	Reflux	150	29
2	0.01	EtOH	Reflux	85	73
3	0.01	EtOH–H_2O (1:1)	Reflux	140	37
4	0.01	EtOH–H_2O (2:1)	Reflux	130	45
5	0.01	EtOH–H_2O (4:1)	Reflux	110	55
6	0.01	Solvent-free	60	65	73
7	0.01	Solvent-free	80	55	82
8	0.01	Solvent-free	100	60	90
9	0.03	Solvent-free	100	120	89
10	0.05	Solvent-free	100	135	88
11	0.07	Solvent-free	100	145	74
12	0.01 ($Fe_{3-x}Ti_xO_4$)	Solvent-free	100	120	53
13	Catalyst-free	Solvent-free	80	180	Trace

[a]Conditions: benzaldehyde (1 mmol), malononitrile (1 mmol), 3-methyl-1-phenyl-1*H*-2-pyrazol-5(4*H*)-one (1 mmol), solvent (5 ml).

[b]Isolated pure yield.

TABLE 2 Synthesis of 1,4-dihydropyrano[2,3-*c*]pyrazoles catalysed by $Fe_{3-x}Ti_xO_4$@TMSP@TBAAsp MNPs under solvent-free conditions at 100°C[a]

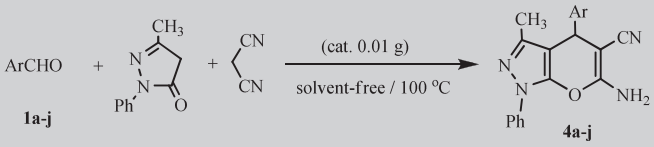

Entry	Ar	Product	Time (min)	Yield (%)[b]	M.p. (°C) Found	M.p. (°C) Reported
1	C_6H_5	**4a**	60	90	170–173	168–170[25]
2	3-$O_2NC_6H_4$	**4b**	40	89	191–193	189–191[33]
3	3-ClC_6H_4	**4c**	20	89	159–162	158–160[33]
4	3-BrC_6H_4	**4d**	15	88	162–165	160–163[22]
5	2,4-$Cl_2C_6H_3$	**4e**	25	89	184–187	185–187[33]
6	4-$MeOC_6H_4$	**4f**	60	88	177–180	177–178[22]
7	4-BrC_6H_4	**4 g**	35	96	190–193	187–189[33]
8	4-MeC_6H_4	**4 h**	45	87	175–178	176–178[34]
9	3-EtO-4-HOC_6H_3	**4i**	30	86	186–190	187–189[33]
10	4-ClC_6H_4	**4j**	20	94	178–181	177–178[34]

[a]Conditions: aldehyde (1 mmol), malononitrile (1 mmol), 3-methyl-1-phenyl-2-pyrazolin-5-one (1 mmol), solvent-free, catalyst (0.01 g), 100 °C.

[b]Isolated pure yield.

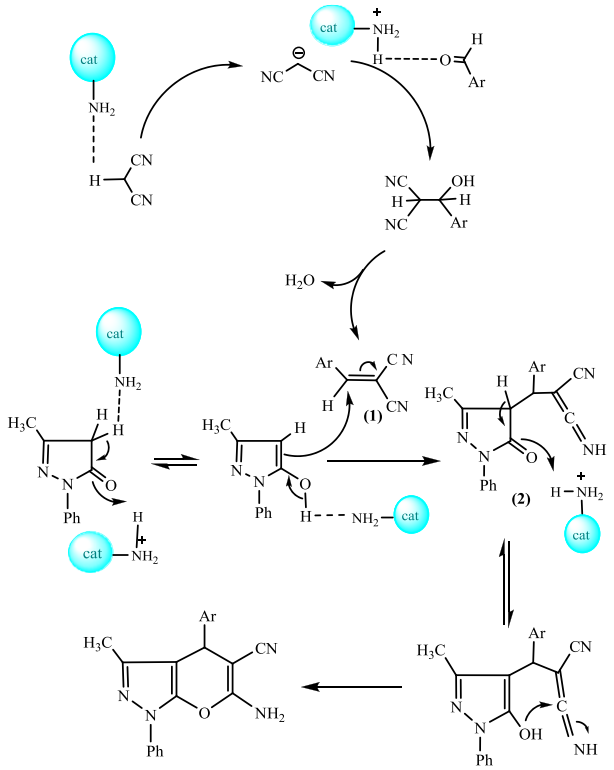

SCHEME 2 Possible mechanism for synthesis of 1,4-dihydro pyrano [2,3-*c*]pyrazoles catalysed by $Fe_{3-x}Ti_xO_4$@TMSP@TBAAsp MNPs

undergoes an addition reaction with the activated aldehyde to produce arylidenemalononitrile intermediate (**1**) after dehydration. Then, nucleophilic addition of 3-methyl-1-phenyl-2-pyrazolin-5-one to intermediate **1** occurs to give intermediate **2**. Finally, tautomerization of intermediate **2** followed by intermolecular cyclization affords the respective product.

3.4 | Catalyst reusability

The reusability potential of the $Fe_{3-x}Ti_xO_4$@TMSP@TBAAsp catalyst was studied in the model reaction between 4-chlorobenzaldehyde, malononitrile and 3-methyl-1-phenyl-2-pyrazolin-5-one under optimal conditions. Once the reaction was completed, the catalyst was magnetically separated, washed with hot ethanol and reused for at least six consecutive runs with no considerable loss of catalyst activity (Table 3).

TABLE 3 Catalytic reusability of $Fe_{3-x}Ti_xO_4$@TMSP@TBAAsp MNPs for synthesis of 1,4-dihydropyrano[2,3-*c*]pyrazole (**4j**)

Run	Time (min)	Yield (%)[a]
1	10	94
2	15	92
3	18	91
4	25	89
5	31	88
6	35	86

[a]Isolated yield.

4 | CONCLUSIONS

In summary, magnetic IL-based aspargine-functionalized $Fe_{3-x}Ti_xO_4$@TMSP@TBAAsp nanoparticles were prepared by a simple procedure using commercially available non-toxic materials and characterized using several analytical techniques. These nanoparticles were probed as an efficient, versatile and selective heterogeneous catalyst for the synthesis of 1,4-dihydropyrano[2,3-*c*]pyrazoles. The high catalytic activity and selectivity, easy magnetic separation and recyclability of the catalyst, low reaction times, high product yields, environmentally friendly solvent-free reaction conditions and simple work-up place the presented catalyst in a unique position as an attractive and promising heterogeneous IL-based nanocatalyst for organic syntheses and transformations.

ACKNOWLEDGEMENT

The authors gratefully acknowledge the financial support granted by the Research Council of Bu-Ali Sina University.

REFERENCES

[1] P. Tartaj, M. P. Morales, S. Veintemillas-Verdaguer, T. Gonzalez-Carreño, C. J. Serna, in *Handbook of Magnetic Materials*, (Ed: K. H. J. Buschow), Elsevier, Amsterdam **2006**, 403.

[2] G. Oskam, J. Sol-Gel, *Sci. Technol.* **2006**, *37*, 161.

[3] W. Wu, Q. G. He, C. Z. Jiang, *Nanoscale Res. Lett.* **2008**, *3*, 397.

[4] I. J. Bruce, T. Sen, *Langmuir* **2005**, *21*, 7029.

[5] R. Sheldon, *Chem. Commun.* **2001**, 2399.

[6] H. Olivier-Bourbigou, L. Magna, D. Morvan, *Appl. Catal. A* **2010**, *373*, 1.

[7] P. Wasserscheid, T. Welton, *Ionic Liquids in Synthesis*, 2nd ed., Wiley, Weinheim **2007**.

[8] J. Safari, Z. Zarnegar, *New J. Chem.* **2014**, *38*, 358.

[9] A. Farrokhi, K. Ghodrati, I. Yavari, *Catal. Commun.* **2015**, *63*, 41.

[10] P.-H. Li, B.-L. Li, H.-C. Hu, X.-N. Zhao, Z.-H. Zhang, *Catal. Commun.* **2014**, *46*, 118.

[11] C. Yuan, Z. Huang, J. Chen, *Catal. Commun.* **2012**, *24*, 56.

[12] Y. Zhu, L. P. Stubbs, F. Ho, R. Liu, C. P. Ship, J. A. Maguire, N. S. Hosmane, *ChemCatChem* **2010**, *2*, 365.

[13] A. Maleki, Z. Alrezvani, S. Maleki, *Catal. Commun.* **2015**, *69*, 29.

[14] F. Zamani, S.-M. Hosseini, *Catal. Commun.* **2014**, *43*, 164.

[15] X. Zheng, S. Luo, L. Zhang, J. P. Cheng, *Green Chem.* **2009**, *11*, 455.

[16] Y. Jiang, C. Guo, H. Xia, I. Mahmood, C. Liu, H. Liu, *J. Mol. Catal. B* **2009**, *58*, 103.

[17] J. Zhu, H. Bienayme, *Multicomponent Reactions*, Wiley-VCH, Weinheim **2005**.

[18] A. Rahmati, N. Pashmforoush, *J. Iran. Chem. Soc.* **2015**, *12*, 993.

[19] F. Shirini, M. Abedini, *J. Nanosci. Nanotechnol.* **2013**, *13*, 4838.

[20] S. G. Kuo, L. J. Huang, H. Nakamura, *J. Med. Chem.* **1984**, *27*, 539.

[21] N. Fawzy, A. Shalaby, M. Zaki, *Molecules* **1998**, *2*, 121.

[22] D. Azarifar, Y. Abbasi, *Synth. Commun.* **2016**, *46*, 745.

[23] M. Babaie, H. Sheibani, *Arabian J. Chem.* **2011**, *4*, 159.

[24] G. Mohammadi-Ziarani, A. Abbasi, A. Badiei, Z. Aslani, *E-J. Chem.* **2011**, *8*, 293.

[25] N. Iravani, M. Keshavarz, H. A. Shojaeian Kish, R. Parandvar, *Chinese J. Catal* **2015**, *36*, 626.

[26] C. R. Allen, P. L. Richard, A. J. Ward, L. G. A. V. Water, A. F. Masters, T. Maschmeyer, *Tetrahedron Lett.* **2006**, *47*, 7367.

[27] X. Liang, Y. Zhong, S. Zhu, L. Ma, P. Yuan, J. Zhu, H. He, Z. Jiang, *J. Hazard. Mater.* **2012**, *199–200*, 247.

[28] D. Azarifar, Y. Abbasi, O. Badalkhani, *J. Iran. Chem. Soc.* **2016**, *13*, 2029.

[29] M. B. Gawande, A. K. Rathi, I. D. Nogueira, R. S. Varma, P. S. Branco, *Green Chem.* **2013**, *15*, 1895.

[30] F. Nemati, M. M. Heravi, R. Saeedi Radi, *Chinese J. Catal.* **2012**, *33*, 1825.

[31] D. Azarifar, O. Badalkhani, Y. Abbasi, M. Hasanabadi, *J. Iran. Chem. Soc.* **2017**, *14*, 403.

[32] U. Chinna Rajesh, Divya, D. S. Rawat, *RSC Adv* **2014**, *4*, 41323.

[33] A. Azarifar, R. Nejat-Yami, M. Al Kobaisi, D. Azarifar, *J. Iran. Chem. Soc.* **2012**, *10*, 439.

[34] D. Shi, J. Mou, Q. Zhuang, L. Niu, N. Wu, X. Wang, *Synth. Commun.* **2004**, *34*, 4557.

SUPPORTING INFORMATION

Additional Supporting Information may be found online in the supporting information tab for this article.

How to cite this article: Azarifar D, Badalkhani O, Abbasi Y. Amino acid ionic liquid-based titanomagnetite nanoparticles: An efficient and green nanocatalyst for the synthesis of 1,4-dihydropyrano[2,3-*c*]pyrazoles. *Appl Organometal Chem*. 2017;e3949. https://doi.org/10.1002/aoc.3949